

## 6.4 Robust Stability

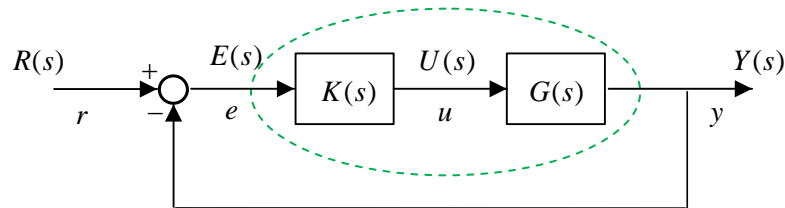


Fig. 7

**Loop Transfer Function:**  $L(s) = G(s)K(s)$

### Essential value of Nyquist's Theorem:

It allows us a direct method of evaluating stability robustness with respect to variations in the loop transfer function variation.

### Gain Margin and Phase Margin for SISO Feedback Control Systems

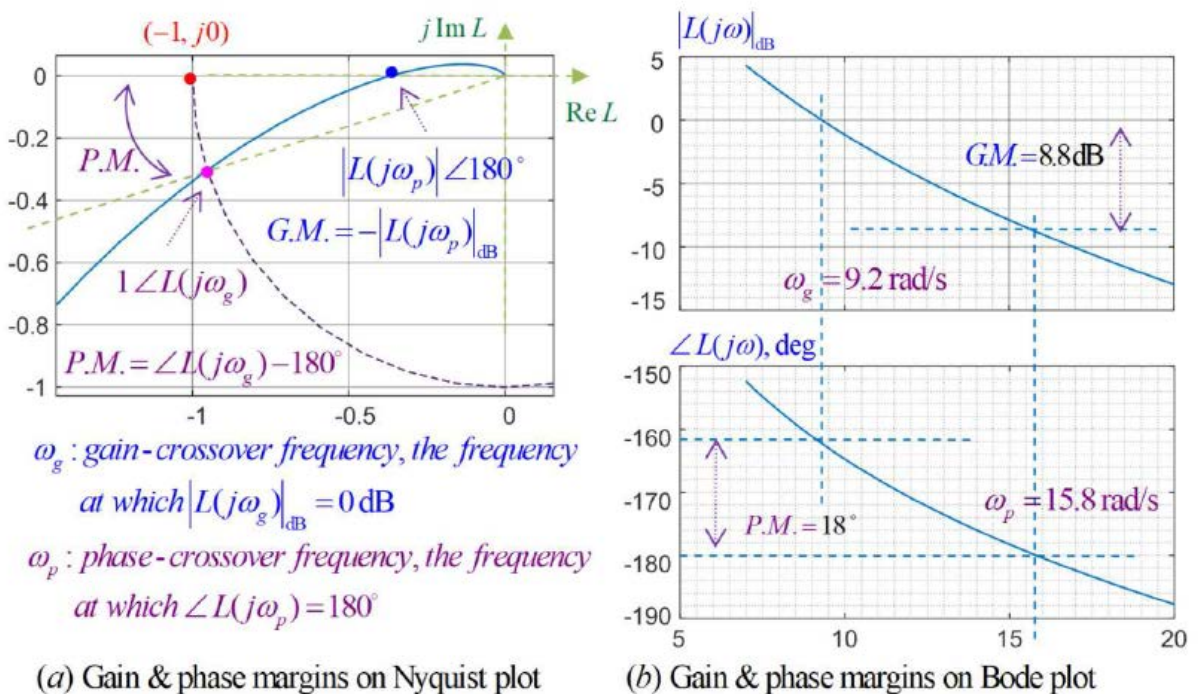


**Fig. 16** Gain and phase margins for SISO feedback control systems

## 6.4.1 Gain and Phase Margins

### Reading Gain Margin from Nyquist Plot

In the partial Nyquist plot of  $L(s)$  shown in *Fig.16(a)*, the **gain margin** is determined by the position of **the intersection (the blue dot) of the Nyquist image  $\Gamma_L$  (the blue curve) and the negative real axis**. The intersection position is represented by the complex number on the  $L$ -plane:

$$|L(j\omega_p)| \angle 180^\circ$$

where  $\omega_p$  is called the **phase-crossover frequency at which the phase of  $L(j\omega_p)$  is  $180^\circ$** . The gain margin is defined by the following equation:

$$GM = -|L(j\omega_p)|_{dB} = -20\log_{10}|L(j\omega_p)| \quad (9.47)$$

If this intersection point is between the origin  $(0, j0)$  and the critical point  $(-1, j0)$  (the red dot), which means the intersection is on the right-hand side of  $(-1, j0)$ , then the magnitude  $|L(j\omega_p)|$  will be less than 1 and the gain margin (GM) will be positive.

A closed-loop system with a positive gain margin does not mean it is stable. However, if the system is stable when the intersection point is between  $(-1, j0)$  and  $(0, j0)$ , then the same system will continue to be stable as long as the intersection point remains inside the interval.

The gain margin is a good indication on how much gain variation is allowed for the system to stay stable. For example, if the intersection is at  $(-0.1, j0)$  or  $0.1 \angle 180^\circ$ , the gain margin will be

$$GM = -20\log_{10}0.1 = 20 \text{ dB}$$

and the system will remain stable if the system gain will not increase to ten times of its original gain. On the other hand, if the intersection point is at  $(-0.8, j0)$  or  $0.8 \angle 180^\circ$ , the gain margin will be

$$GM = -20\log_{10}0.8 = 1.94 \text{ dB}$$

and the system gain will only need to increase by 25% (or become 1.25 times of its original value) to move the intersection point to the other side of the critical point  $(-1, j0)$  to destabilize the system. If the intersection point moves to the other side of the critical point  $(-1, j0)$ , the number of encirclements of  $(-1, j0)$  by the Nyquist image contour will change; hence, the stability status of the closed-loop system will change according to the Nyquist stability criterion.

Therefore, the system will be more stable if the absolute value of gain margin is larger, or if the intersection point  $|L(j\omega_p)| \angle 180^\circ$  is further away from the critical point  $(-1, j0)$ .

## Reading Gain Margin from Bode Plot

Although the Nyquist plot clearly shows the intersection point of the Nyquist image  $\Gamma_L$  with the negative real axis, it does not reveal the phase-crossover frequency. Since the Bode plot explicitly show both the magnitude and the phase of  $L(j\omega)$  as functions of the frequency, they provide more detailed information.

As defined, the gain margin is determined by the magnitude of  $|L(j\omega_p)| \angle 180^\circ$ . The phase-crossover frequency,  $\omega_p$ , is the frequency at which the phase of  $L(j\omega)$  is  $180^\circ$  or  $-180^\circ$ . From the Bode plot shown in Fig.16(b), it is easy to see that the  $\angle L(j\omega)$  phase curve intersects the  $-180^\circ$  horizontal line when the frequency  $\omega$  is the phase-crossover frequency  $\omega_p$ . Draw a vertical straight line at the phase-crossover frequency,  $\omega_p = 15.8$  rad/s, and extend this line up to intersect the  $|L(j\omega)|_{dB}$  magnitude curve. Then, the value of  $|L(j\omega)|_{dB}$  at  $\omega_p = 15.8$  rad/s can be read from the graph as  $|L(j\omega_p)|_{dB} = -8.8$  dB. Therefore, the gain margin is

$$GM = -|L(j\omega_p)|_{dB} = 8.8 \text{ dB}$$

## Reading Phase Margin from Nyquist Plot

In the partial Nyquist plot of  $L(j\omega)$ , shown in Fig.16(a), the phase margin is determined by the intersection (the purple dot) of the Nyquist image  $\Gamma_L$  and the unit circle centered at the origin. The intersection position is represented by the complex number on the  $L$ -plane

$$1 \angle L(j\omega_g)$$

where  $\omega_g$  is called the **gain-crossover frequency at which the magnitude of  $L(j\omega_g)$  is one, or  $|L(j\omega_g)|_{dB} = 0\text{dB}$** . The phase margin is defined by the following equation:

$$PM = \angle L(j\omega_g) - 180^\circ$$

Just like the perturbation of the gain, the variation of the phase of the loop transfer function  $L(s)$  can also destabilize a system. Recall that in Section 6.3.4, a time delay will cause a phase lag in the Nyquist plot of  $L(s)$ . **A system with larger absolute value of phase margin will be more robust against the phase variations of the system.**

## Reading Phase Margin from Bode Plot

As defined, the phase margin is determined by the phase of  $L(j\omega)$  at the gain-crossover frequency  $\omega_g$ , the frequency at which the magnitude of  $L(j\omega_g)$  is 1 or  $|L(j\omega_g)|_{dB} = 0\text{dB}$ . The first step is to find the gain-crossover frequency  $\omega_g$ . From the Bode plot shown in Fig.16(b), it is easy to see that **the intersection of the  $|L(j\omega)|_{dB}$  curve with the 0 dB horizontal line on the magnitude plot occurs when the frequency  $\omega$  is the gain-crossover frequency  $\omega_g$** . Draw a vertical straight line at the gain-crossover frequency,  $\omega_g = 9.2$  rad/s, and extend this line down to the phase plot to intersect the  $\angle L(j\omega)$  curve. The value of  $\angle L(j\omega_g)$  at  $\omega_g = 9.2$  rad/s can be read from the phase plot that  $\angle L(j\omega_g)$  is  $-162^\circ$ . Therefore, the phase margin is  $PM = -162^\circ - 180^\circ = 18^\circ$ .

### 6.4.2 Effect of the Gain of Loop Transfer Function on Gain and Phase Margins

#### Ex 11: Stabilize an Originally Unstable System to a Desired Gain Margin

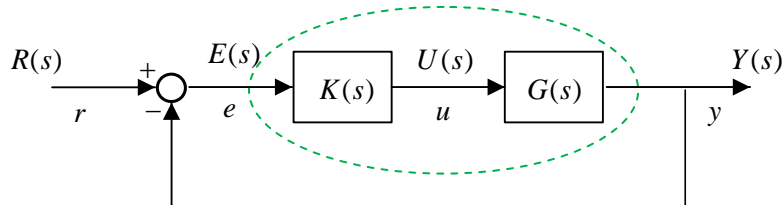
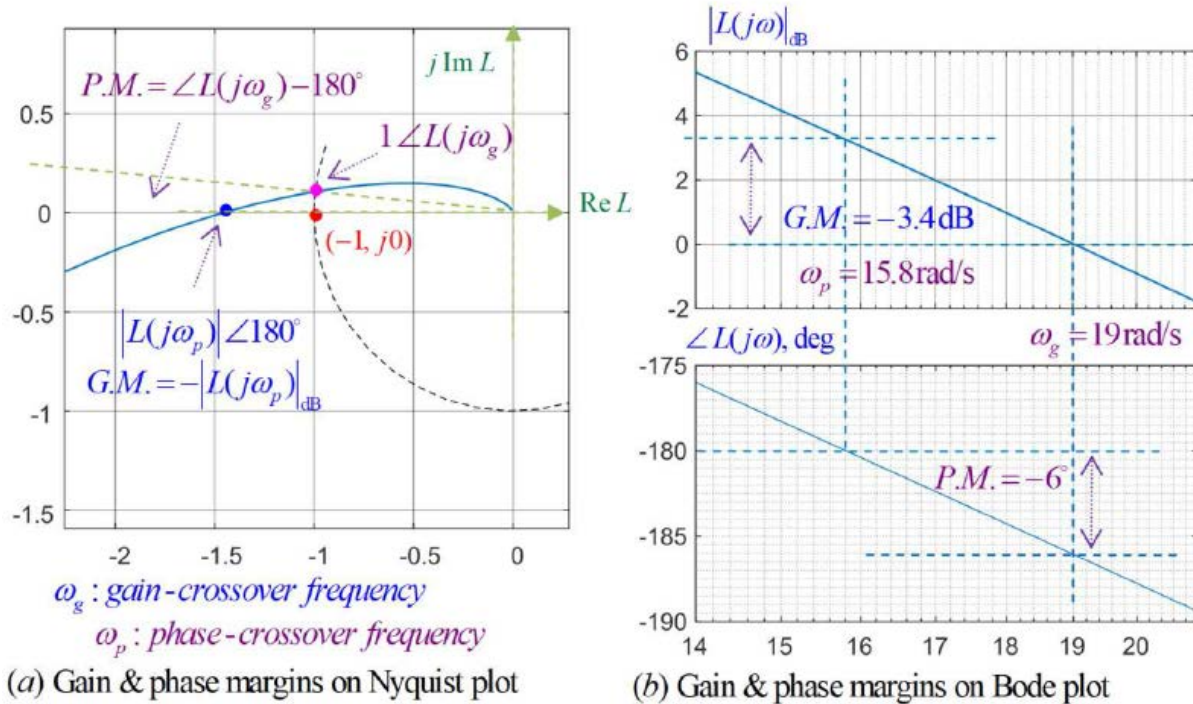


Fig. 7

**Loop Transfer Function:**  $L(s) = G(s)K(s) = \frac{20000}{s^3 + 55s^2 + 250s}$



**Fig. 17 The gain and phase margins of the unstable system in Ex. 11**

From the partial Nyquist plot and the Bode plot in Fig.17(a) and 17(b), respectively, we have found the gain and phase margins of the system as follows:

$$GM = -|L(j\omega_p)|_{dB} = -3.4 \text{ dB} \quad \text{where} \quad \omega_p = 15.8 \text{ rad/s}$$

$$P.M. = \angle L(j\omega_g) - 180^\circ = -6^\circ \quad \text{where} \quad \omega_g = 19 \text{ rad/s}$$

Note that the system has negative gain and phase margins, since the Nyquist image  $\Gamma_L$  intersects the negative real axis at the left-hand side of the critical point  $(-1, j0)$ . In general, a system with negative gain or phase margin does not mean the closed-loop system is unstable. The information given by the partial Nyquist plot and the Bode plot is not enough to determine if the closed-loop system is stable.

However, it is quite straightforward to check the closed-loop stability by solving the three roots of the characteristic equation or using the Routh-Hurwitz criterion, or the Nyquist stability criterion based on the complete Nyquist plot. The system is indeed unstable, but both the gain and phase margins are small.

A gain margin of  $-3.4$  dB means that it only requires a small gain reduction of  $L(s)$  to 67% of its original gain to stabilize the closed-loop system.

Assume the loop transfer function  $L(s)$  structure is slightly modified to

$$L(s) = \frac{20000K}{s^3 + 55s^2 + 250s}$$

where  $K$  is a constant gain to be designed. The system is the same as the original one if  $K = 1$ .

In general, this  $K$  can be a function of  $s$ , or  $K(j\omega)$  is a function of frequency  $\omega$ , so that the system can be designed to satisfy multiple design objectives like robust stability, disturbance reduction, and control-input constraints.

Here, we will assume  $K$  is just a constant parameter to be determined so that a robust stability objective can be achieved.

Now the closed-loop system is unstable with gain margin  $-3.4$  dB and phase margin  $-6^\circ$ . We would like to design a simple constant controller  $K$  so that the closed-loop system is stable with gain margin improved to 14.6 dB.

Since the change of  $K$  will not affect the phase, the phase plot will remain the same. From the Bode plot in Fig.18(b), it can be seen that the gain and phase margins will improve if the  $|L(j\omega)|_{dB}$  curve is moved down on the magnitude plot while the phase plot remains unchanged.



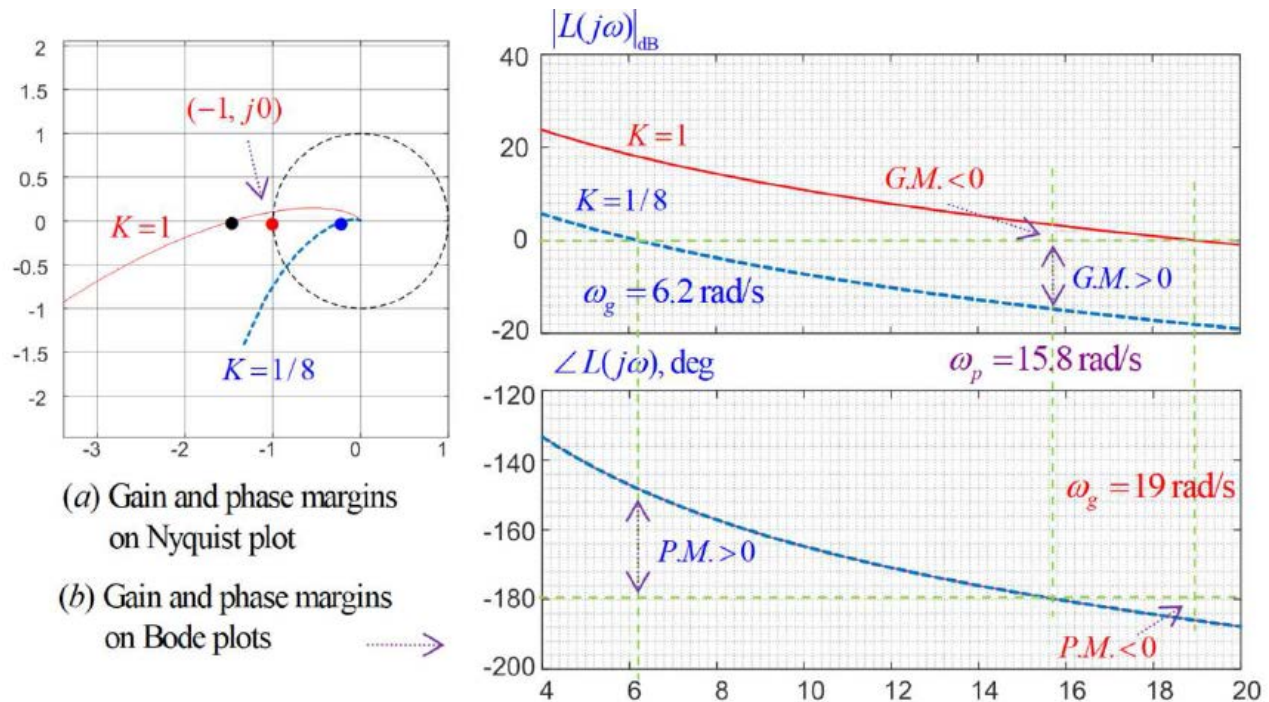


**Fig. 18 Illustration of reducing  $K$  to move down the  $|L(j\omega)|_{dB}$  curve to improve the gain and phase margins of an originally unstable closed-loop system in Ex.11.**

The graphs in Fig.18(a) and (b) show the differences between the original system (with  $K = 1$ ) and the modified system (with  $K = 1/8$ ) in the Nyquist plot and in the Bode plot. **The Nyquist plot shows that the Nyquist image  $\Gamma_L$  has moved its intersection point** with the negative real axis from the black dot position, crossing over the red dot critical point  $(-1, j0)$ , to become stable toward the blue dot position.

The Nyquist plot shows clearly that an obvious robust stability improvement has been achieved, but it does not reveal the details quantitatively.

The Bode plot shows clearly that if the objective is to achieve a gain margin of 14.6 dB, then  **$K$  needs to be reduced to a level so that the  $|L(j\omega)|_{dB}$  curve can move down by 18 dB on the magnitude plot.** The 18 dB reduction of gain is approximately equivalent to reducing  $K$  from 1 to  $1/8$ .

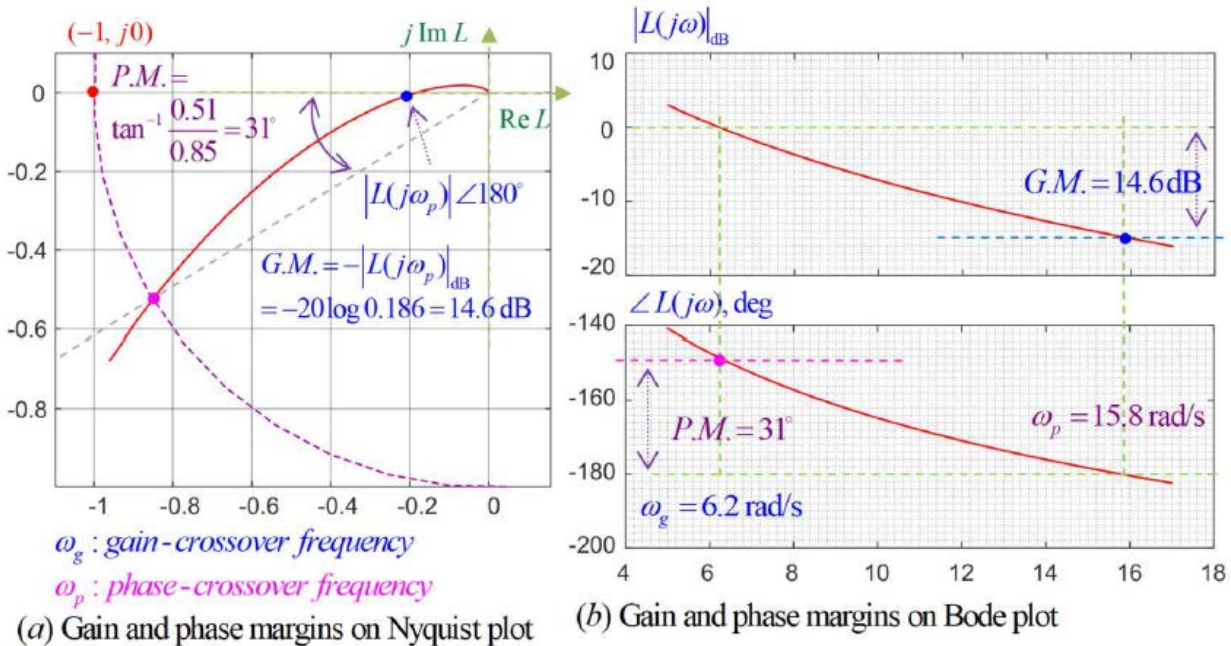


**Fig. 19** Illustration of reducing  $K$  to from 1 to  $1/8$  to improve the gain margin by 18 dB and the phase margin by  $37^\circ$  in Ex 11.

With  $K = 1/8$ , the Nyquist plot and the Bode plot have been modified to those shown in Fig.19(a) and (b), respectively. It can be seen that the phase-crossover frequency is still at  $\omega_p = 15.8$  rad/s, but due to the 18 dB reduction of  $|L(j\omega)|_{dB}$ , the gain margin has improved from  $-3.4$  dB to 14.6 dB. Although the phase plot remains unchanged, the gain-crossover frequency has changed from  $\omega_g = 19$  rad/s to  $\omega_g = 6.2$  rad/s, and the phase margin has improved from  $-6^\circ$  to  $31^\circ$ .

In the following example, we will revisit the system considered in Ex. 7. The system has a double-crossing Nyquist image that intersects the negative real axis twice. According to Nyquist stability criterion, the closed-loop system will be stable when these two intersections are at the opposite sides of the critical point  $(-1, j0)$ . Furthermore, the gain margins are determined by the two intersection positions. The gain margin for the intersection on the right is positive while the other has a negative gain margin.



## Ex 12: A System with Double-crossing Nyquist Image Has Positive and Negative Gain Margins at the Same Time

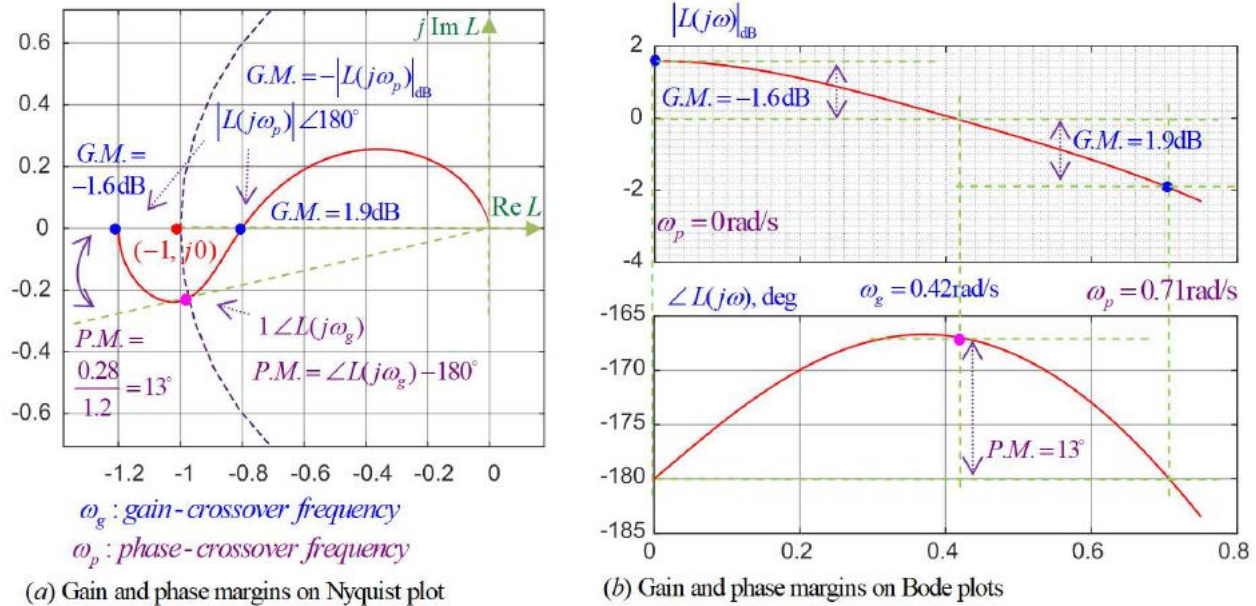


**Fig. 20** Revisit the double-crossing Nyquist image of Ex.7 that has positive and negative gain margins at the same time.

The system considered in Ex 7 has a double-crossing Nyquist image, as shown in Fig.11. Its loop transfer function is

$$L(s) = \frac{0.6K}{(s - 0.5)(s^2 + s + 1)}$$

A partial Nyquist plot and the Bode plot of  $L(s)$  with  $K = 1$  are shown in Fig.20(a) and (b), respectively. **Note that the Nyquist image  $\Gamma_L$  intersects the negative real axis of the  $L$ -plane at the following two points:**

$$L(j0) = -1.2 \quad \text{and} \quad L(j\sqrt{0.5}) = -0.8$$

It has been shown in Ex. 7 that the system is stable. According to the definition of gain and phase margins, the system has a phase margin  $PM = 13^\circ$  but has two gain margins

$$GM_1 = -20\log_{10}0.8 = 1.9382 \text{ dB} \quad \text{and} \quad GM_2 = -20\log_{10}1.2 = -1.5836 \text{ dB}$$

The positive gain margin on the right is  $GM_1 = 1.9382\text{dB}$ . It means that the gain of the loop transfer function  $K$  is allowed to increase to  $K = 1.25$  without destabilizing the closed-loop system.

On the other hand, the negative gain margin  $GM_2 = -1.5836\text{dB}$  indicates that the closed-loop system can stay stable as long as  $K$  is not reduced to below  $K = 5/6$ . In other words, the closed-loop system is stable if and only if

$$5/6 < K < 1.25$$

Note that the stability range of  $K$  derived in terms of the two gain margins is consistent with the inequality in [Ex 7](#), which was found based on the Nyquist stability criterion.

## 6.5 Generalized Stability Margins

As described in the previous section, the gain and phase margins are good indications of how much gain perturbation is allowed at the phase-crossover frequency and how much phase variation is permitted at the gain-crossover frequency, respectively.

However, these two stability margin measures only reveal the robust stability information at two frequencies, not the whole frequency spectrum.

Furthermore, these two measures only work for SISO (single-input/single-output) systems.

The attempt of extending the concept of robust stability margins to MIMO (multi-input, multi-output) systems was not successful until 1966 when the small gain theorem was discovered.

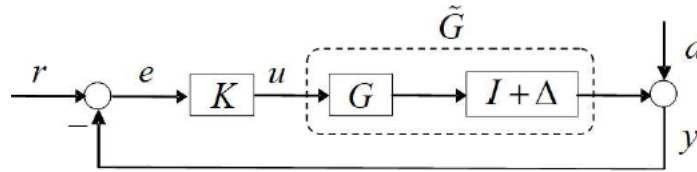


**Fig. 21 A typical feedback control system with unstructured norm-bounded plant uncertainties.**

### 6.5.1 Small Gain Theorem and Robust Stability

Consider the feedback control system with plant uncertainties shown in *Fig.21*. The nominal plant model is represented by  $G$ , and the set of uncertain plants is described by

$$\mathcal{G} = \left\{ \tilde{G} : \tilde{G} = (I + \Delta)G, \text{ where } \Delta(s) \in RH_{\infty} \text{ and } \bar{\sigma}[\Delta(j\omega)] \leq \ell(\omega) \right\} \quad (9.53)$$

Here,  $RH_{\infty}$  represents the set of rational function matrices with real coefficients that are analytic (have no poles) in the closed right half complex plane, and  $\bar{\sigma}[X]$  stands for the maximum singular value of  $X$ , or, equivalently, the square root of the maximum eigenvalue of  $X^*X$ , where  $X^*$  is the conjugate transpose of the complex matrix  $X$ .

**The positive real scalar function  $\ell(\omega)$  prescribes the maximum magnitude variation of the uncertain plant dynamics at all frequencies** according to the practical system and its working environment. In reality, the discrepancy between the nominal model and the real system is larger at higher frequencies, and, thus, extra care needs to be given for high-frequency uncertainties in dealing with robust stability issues.

The unstructured plant uncertainties include unmodeled dynamics and any variation caused by environmental parameters, which are unknown except the bounded norm information in  $\ell(\omega)$ . To determine a necessary and sufficient condition so that the uncertain closed-loop system is stable seems to be a very difficult problem.

Surprisingly, this challenging robust stability design problem was solved in an effective and elegant fashion, as shown below in the **Small Gain Theorem**.

## Sensitivity and Complementary Sensitivity Functions

Consider the feedback control system shown in *Fig.21*, where  $G$  and  $\tilde{G}$  are the nominal and the perturbed models of the system to be controlled, respectively, and  $\Delta$  represents a set of plant uncertainties.

In general, the controller  $K$  is designed so that the closed-loop system has desired performance. There are two closed-loop transfer functions that are central to understanding the performance of feedback systems. **These are the sensitivity function,  $S(s)$ , and the complementary sensitivity function,  $T(s)$ . Let the loop transfer function (LTF) be denoted by**

$$L(s) = G(s)K(s) \quad (9.54)$$

**and define**

$$S(s) = [I + L(s)]^{-1} \quad \text{and} \quad T(s) = L(s)[I + L(s)]^{-1} \quad (9.55)$$

For the feedback control system of *Fig.21*, if  $\Delta = 0$  and  $d = 0$ , where  $d$  is the disturbance input, then the relationship between the reference input  $R(s) = \mathcal{L}[r(t)]$  and **the tracking error  $E(s) = \mathcal{L}[e(t)]$  is**

$$E(s) = [I + L(s)]^{-1}R(s) = S(s)R(s)$$

**Thus, a smaller  $S(s)$  will lead to a smaller tracking/regulation error. Similarly, if  $\Delta = 0$  and  $r = 0$ , then the relationship between the disturbance input  $D(s) = \mathcal{L}[d(t)]$  and the output disturbance response  $Y(s) = \mathcal{L}[y(t)]$  is**

$$Y(s) = [I + L(s)]^{-1} D(s) = S(s) D(s)$$

**Hence, a smaller  $S(s)$  will also imply a smaller disturbance response.**

**On the other hand, as will be seen in the Small Gain Theorem below that a smaller complementary sensitivity function  $T(s)$  will produce better robust stability.**

**Therefore, to achieve smaller tracking/regulation error, less disturbance response, and better robust stability, the controller needs to be designed so that the sensitivity function and the complementary sensitivity function are both small, if possible.**

**However, it is impossible to reduce both at the same time and at the same frequency since the sum of  $S(s)$  and  $T(s)$  is a constant:**

$$S(s) + T(s) = [I + L(s)]^{-1} + L(s)[I + L(s)]^{-1} = [I + L(s)][I + L(s)]^{-1} = I$$

**Nevertheless, plant uncertainties are more significant in high frequency range than low frequencies while the disturbances and the reference inputs usually occur in low frequency range. Therefore, the controller can be designed to minimize  $|S(j\omega)|$  in low frequency range while reducing  $|T(j\omega)|$  at high frequencies.**



### Theorem 3: Small Gain Theorem for Robust Stability

Consider the feedback control system with plant uncertainty described by the block diagram shown in Fig.21 and by the set of uncertain plants satisfying the bounded norm condition described in Equation 9.53. The loop transfer function matrix  $L(s)$  and the complementary sensitivity function matrix  $T(s)$  of the nominal closed-loop system are defined in Equations 9.54 and 9.55, respectively.

*If the nominal closed-loop system  $\mathcal{C}(G, K)$ , which is the closed-loop system with  $\Delta = 0$  or  $\tilde{G} = G$ , is stable, then the uncertain closed-loop system  $\mathcal{C}(\tilde{G}, K)$  is stable if and only if the following inequality is satisfied:*

$$\bar{\sigma}[T(j\omega)] < \frac{1}{\ell(\omega)} \quad \text{for all } \omega \quad (9.56)$$

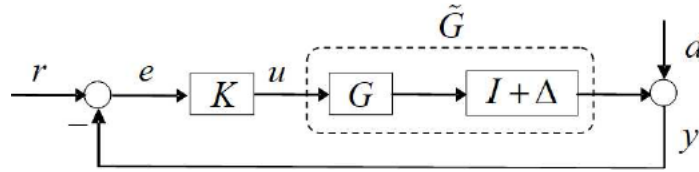


**Fig. 21 A typical feedback control system with unstructured norm-bounded plant uncertainties.**

$$\mathcal{G} = \left\{ \tilde{G} : \tilde{G} = (I + \Delta)G, \text{ where } \Delta(s) \in RH_{\infty} \text{ and } \bar{\sigma}[\Delta(j\omega)] \leq \ell(\omega) \right\} \quad (9.53)$$

$$L(s) = G(s)K(s) \quad (9.54)$$

$$S(s) = [I + L(s)]^{-1} \quad \text{and} \quad T(s) = L(s)[I + L(s)]^{-1} \quad (9.55)$$

### Corollary 3: Special Case of the Small Gain Theorem for SISO Systems

Consider the same feedback control system with plant uncertainties described by Fig.21 and Equation 9.53 except that all matrix functions are replaced by their scalar function counterparts and  $\bar{\sigma}[\Delta(j\omega)] \leq \ell(\omega)$  is regarded as

$$|\Delta(j\omega)| \leq \ell(\omega)$$

Then the uncertain closed-loop system  $\mathcal{C}(\tilde{G}, K)$  is stable if and only if the following inequality is satisfied:

$$|T(j\omega)| < \frac{1}{\ell(\omega)} \quad \text{for all } \omega \quad (9.57)$$

#### 6.5.2 Interpretation of the Generalized Stability Margins

As described in Section 6.5.1, we learned that a generalized frequency-dependent stability margin function can be obtained from the small gain theorem. The uncertain closed-loop system  $\mathcal{C}(\tilde{G}, K)$  is stable if and only if

$$|T(j\omega)| < \frac{1}{\ell(\omega)} \quad \text{where} \quad |\Delta(j\omega)| \leq \ell(\omega) \quad \text{for all } \omega$$

For example, if  $|T(j\omega_1)| = 0.5$ , then the maximum allowable variation of  $|T(j\omega_1)|$  has to be less than 2. Otherwise, the system will become unstable.

To guarantee the closed-loop system to be robustly stable, the maximum allowable variation of  $|\Delta(j\omega)|$  has to be less than  $1/|T(j\omega)|$  for all  $\omega$ .

Hence, a generalized stability margin function  $\mathcal{M}(\omega)$  can be defined as follows:

$$\mathcal{M}(\omega) = 1 / \bar{\sigma}[T(j\omega)] = 1 / |T(j\omega)| \quad (9.58)$$

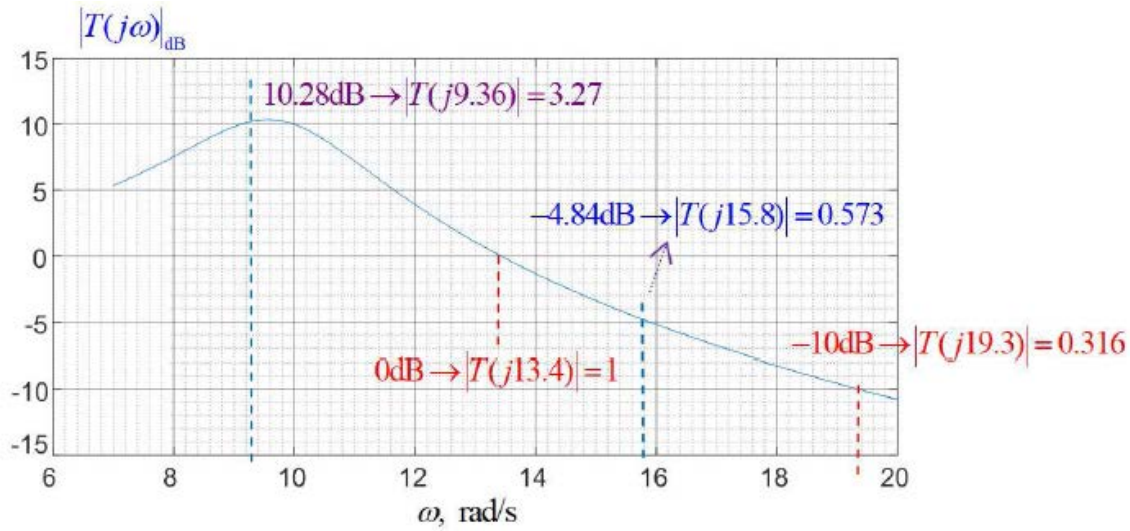


**Fig. 22** The generalized stability margin function  $\mathcal{M}(\omega)$  is the inverse of  $|T(j\omega)|$

### Ex 13: Generalized Stability Margin Function $\mathcal{M}(\omega)$ and $|T(j\omega)|$

Consider the feedback control system with plant uncertainties shown in Fig.21. The loop transfer function of the system is given as

$$L(s) = G(s)K(s) = \frac{5000}{s(s^2 + 55s + 250)}$$

The complementary sensitivity function of the system is

$$T(s) = L(s)[I + L(s)]^{-1}$$

and the magnitude plot of  $T(j\omega)$ ,  $|T(j\omega)|_{dB}$ , is obtained, as shown in Fig.22.

On this complementary sensitivity plot, it can be seen that at  $\omega = 9.36$  rad/s, we have

$$|T(j9.36)|_{dB} = 10.28 \text{ dB} \rightarrow |T(j9.36)| = 3.27 \rightarrow \mathcal{M}(9.36) = 1 / 3.27 = 0.306$$

which means that the maximum allowable magnitude variation of  $|\Delta(j9.36)|$ , to avoid destabilizing the system, is 0.306. If the variation of  $|\Delta(j9.36)|$  is more than 0.306, the system will become unstable.

Similarly, the values of  $T(j\omega)$  at  $\omega = 13.4$  rad/s,  $\omega = 15.8$  rad/s, and  $\omega = 19.3$  rad/s are computed respectively as follows:

$$\begin{aligned} |T(j13.4)|_{\text{dB}} = 0 \text{ dB} &\rightarrow |T(j13.4)| = 1 \rightarrow \mathcal{M}(13.4) = 1/1 = 1 \\ |T(j15.8)|_{\text{dB}} = -4.84 \text{ dB} &\rightarrow |T(j15.8)| = 0.573 \rightarrow \mathcal{M}(15.8) = 1/0.573 = 1.745 \\ |T(j19.3)|_{\text{dB}} = -10 \text{ dB} &\rightarrow |T(j19.3)| = 0.316 \rightarrow \mathcal{M}(19.3) = 1/0.316 = 3.165 \end{aligned}$$

**Therefore, the maximum allowable magnitude variations of  $|\Delta(j\omega)|$  at these three frequencies so that the system will remain stable are  $|\Delta(j13.4)| = 1$ ,  $|\Delta(j15.8)| = 1.745$ , and  $|\Delta(j19.3)| = 3.165$ , respectively.**

**Note that a smaller  $|T(j\omega)|$  allows more magnitude perturbation at that frequency, and the generalized stability margin function is the reciprocal of the magnitude of the complementary sensitivity function. It is also observed that  $|T(j\omega)|$  is decreasing at the high frequency region, which means the high frequency components of the system are allowed larger uncertainties.**

**$\bar{\sigma}[T(j\omega)]$  (or  $|T(j\omega)|$ ) provides important stability margin information for the whole frequency spectrum.**

### 6.5.3 Relationship Between Gain/Phase Margins and the Generalized Stability Margins

In the following we will show that the gain and phase margins can be computed based on the magnitude of the complementary sensitivity function  $|T(j\omega)|$ .

**Theorem 4: Use  $|T(j\omega_p)|$  and  $|T(j\omega_g)|$  to Compute the Gain and Phase Margins**

*Consider the feedback control system in Fig.21 with the loop transfer function  $L(s) = G(s)K(s)$  and the complementary sensitivity function*

$$T(s) = L(s)[I + L(s)]^{-1}.$$

*Assume  $\omega_p$  and  $\omega_g$  are the phase-crossover frequency and the gain-crossover frequency, respectively. Then the gain margin (GM) and the phase margin (PM) of the system can be computed using  $|T(j\omega_p)|$  and  $|T(j\omega_g)|$ .*

(a) If  $|L(j\omega_p)| < 1$ , the gain margin is

$$GM = 20\log_{10} (1 + 1/|T(j\omega_p)|) \quad (9.60)$$

(b) If  $|L(j\omega_p)| > 1$ , the gain margin is

$$GM = 20\log_{10} (1 - 1/|T(j\omega_p)|) \quad (9.61)$$

(c) If  $\angle L(j\omega_g) > \pi$ , the phase margin is

$$PM = 2\sin^{-1} (0.5/|T(j\omega_g)|) \quad (9.62)$$

(d) If  $\angle L(j\omega_g) < \pi$ , the phase margin is

$$PM = -2\sin^{-1} (0.5/|T(j\omega_g)|) \quad (9.63)$$



### Ex 14: The Magnitude Plot of the Complementary Sensitivity Function and Its Relationship with the Gain and Phase Margins

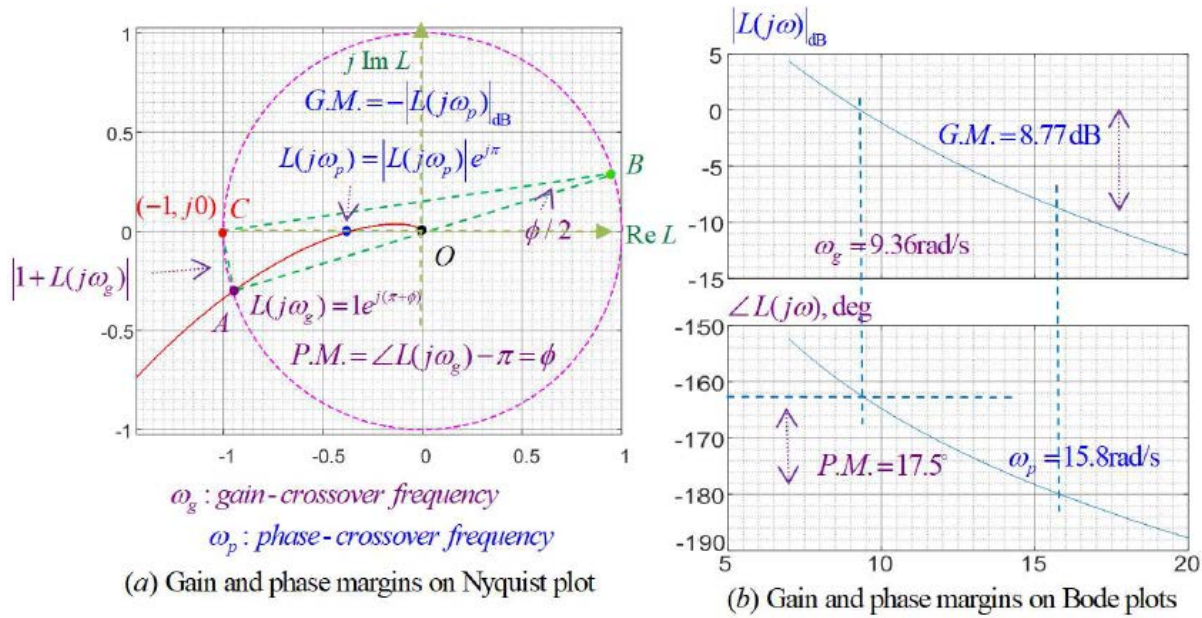


**Fig. 23** Gain and phase margins on Nyquist and Bode plots.

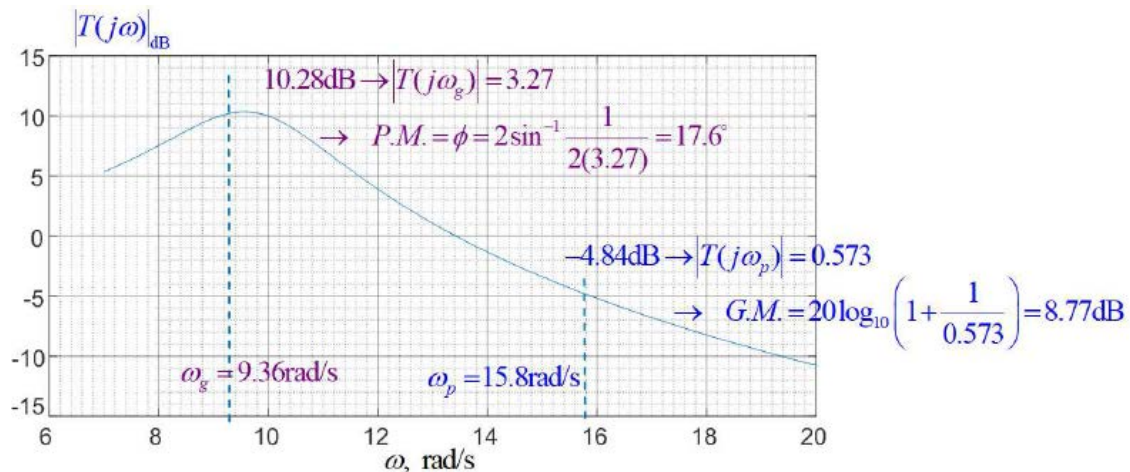


**Fig. 24** Gain and phase margins on the  $|T(j\omega)|$  plot.

The system considered in Ex 13 with the loop transfer function:

$$L(s) = G(s)K(s) = \frac{5000}{s(s^2 + 55s + 250)}$$

is employed in this example to compare the Nyquist plot, Bode plot, and the magnitude plot of  $T(j\omega)$ , which is the complementary sensitivity function,

and to identify the relationship among the gain margin  $GM$ , the phase margin  $PM$ , the magnitude of the complementary sensitivity function  $|T(j\omega)|$ , and the generalized stability margin function  $\mathcal{M}(\omega)$ .

From Fig.23, we have the gain-crossover frequency  $\omega_g = 9.36$  rad/s at which

$$L(j\omega_g) = 1e^{j(\pi+\phi)}$$

and the phase margin is  $PM = \phi = 17.5^\circ$ . The phase-crossover frequency is  $\omega_p = 15.8$  rad/s at which we have  $L(j\omega_p) = |L(j\omega_p)|e^{j\pi}$  and the gain margin can be found as  $GM = -20\log_{10}|L(j\omega_p)| = 8.77$  dB.

The plot of  $|T(j\omega)|$ , the magnitude of the complementary sensitivity function, is shown in Fig.24. As discussed in Ex 13, this magnitude function  $|T(j\omega)|$  is the reciprocal of the generalized stability margin function  $\mathcal{M}(\omega)$ , which specifies the maximum allowable variations of  $\Delta(j\omega)$  for each  $\omega$  so that the system can remain stable.

In Fig.24, when the frequency is at  $\omega = \omega_g$ , the gain-crossover frequency, we have  $|T(j\omega_g)|_{\text{dB}} = 10.28$  dB, which gives  $|T(j\omega_g)| = 3.27$  and its reciprocal, the generalized stability margin function  $\mathcal{M}(\omega_g) = 1 / 3.27 = 0.306$ . This 0.306 stability margin at the frequency  $\omega_g$  means that the variation of  $\Delta(j\omega_g) < 0.306$  will not cause the system to become unstable. In addition to this robust stability information regarding the maximal variation of  $\Delta(j\omega_g)$ , the  $|T(j\omega_g)| = 3.27$  value can be employed to compute the phase margin, as promised by Theorem 4. Plugging  $|T(j\omega_g)| = 3.27$  into Equation 9.62, we have the phase margin

$$PM = \phi = 2\sin^{-1}\left(\frac{0.5}{|T(j\omega_g)|}\right) = 2\sin^{-1}\left(\frac{0.5}{3.27}\right) = 17.6^\circ$$

which is consistent with the result obtained from the Bode plot.

At the frequency  $\omega_p$ , the phase-crossover frequency, we have

$|T(j\omega_p)|_{\text{dB}} = -4.84 \text{ dB}$ , which gives  $|T(j\omega_p)| = 0.573$ . The reciprocal of this,

$\mathcal{M}(\omega_p) = 1 / 0.573 = 1.745$ , is the generalized stability margin. This 1.745

stability margin at the frequency  $\omega_p$  means that the variation of

$\Delta(j\omega_p) < 1.745$  will not destabilize the system. The  $|T(j\omega_p)| = 0.573$  value can be employed to compute the gain margin using Equation 9.60,

$$GM = 20 \log_{10} (1 + 1/|T(j\omega_p)|) = 20 \log_{10} (1 + 1.745) = 8.77 \text{ dB}$$

which is consistent with the result obtained from the Bode plot.

## 6.6 Essential Closed-Loop Transfer Functions and Loop Shaping

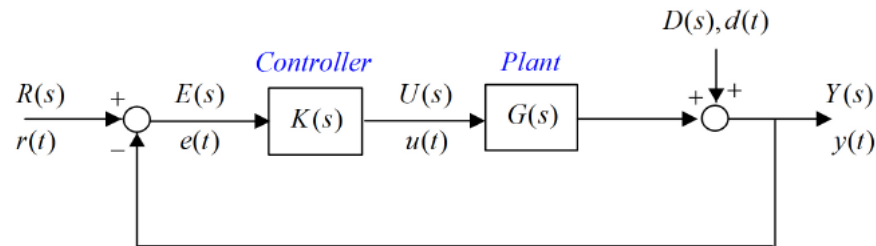


**Fig. 25 A typical feedback control system structure.**

**The complementary sensitivity function**

$$T(s) = L(s)[1 + L(s)]^{-1}$$

where  $L(s) = G(s)K(s)$  is the loop transfer function (LTF) of the closed-loop system, as shown in Fig.25.

**The sensitivity function**

$$S(s) = [1 + L(s)]^{-1}$$

**Recall that a smaller  $S(s)$  will lead to a smaller tracking/regulation error and smaller disturbance response.**

**On the other hand, a smaller complementary sensitivity function  $T(s)$  will produce better robust stability.**

**Design a controller  $K(s)$  so that both of  $S(s)$  and  $T(s)$  are small ?**

$$S(s) + T(s) = [I + L(s)]^{-1} + L(s)[I + L(s)]^{-1} = [I + L(s)][I + L(s)]^{-1} = I$$

**➔ it is impossible to reduce both at the same time and at the same frequency.**

However, it is doable to design a controller so that the sensitivity function  $S(j\omega)$  is small in the low frequency range, while keeping the complementary sensitivity function  $T(j\omega)$  small in the high frequency range.

This control system design is called a **loop shaping approach**.

At low frequencies, the magnitude of the loop transfer function,  $|L|$ , usually is much greater than 1 so that the sensitivity function  $S = (1 + L)^{-1}$  is approximately equal to  $L^{-1}$ ; hence, we have

$$|L(j\omega)| \approx \frac{1}{|S(j\omega)|} \quad \text{at low frequencies when } |L| \gg 1$$

On the other hand, at the high frequency region, the magnitude of the loop transfer function,  $|L|$ , is much less than 1 so that the complementary sensitivity function  $T = L[I + L]^{-1}$  is approximately equal to  $L$ ; hence, we have

$$|L(j\omega)| \approx |T(j\omega)| \quad \text{at high frequencies when } |L| \ll 1$$

Therefore, the loop shaping design can be accomplished by choosing a controller  $K(s)$  so that the magnitude of the loop transfer function  $L(s) = G(s)K(s)$  is large in the low frequency range, but small at high frequencies.

Recall that in Ex 13 and Ex 14, we selected a controller  $K(s)$  to manipulate the loop transfer function  $L(s) = G(s)K(s)$ , and thus the complementary sensitivity function  $T = L[I + L]^{-1}$ , to achieve a desired robust stability requirement.

In the following, we will evaluate the tracking error and disturbance response performance of the system in terms of the sensitivity function  $S = (1 + L)^{-1}$ .



## Ex 15: Loop Shaping for Tracking Performance and Robust Stability

The system considered in Ex 13 with loop transfer function:

$$L(s) = G(s)K(s) = \frac{5000}{s(s^2 + 55s + 250)}$$

is revisited in the following to reveal the **tracking performance** and the **robust stability margin** on the same loop shaping diagram.

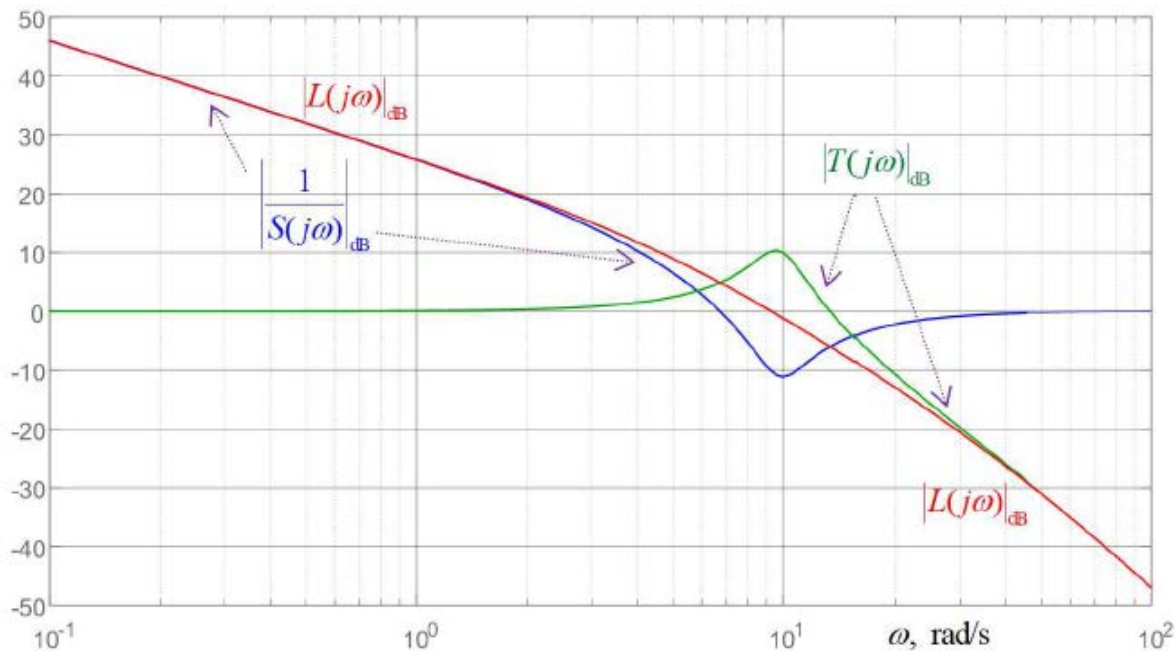


**Fig. 26** A loop shaping diagram showing  $|T(j\omega)|_{dB}$ ,  $|1/S(j\omega)|_{dB}$ , and  $|L(j\omega)|_{dB}$ .

Three graphs —  $|1/S(j\omega)|_{dB}$  in blue,  $|T(j\omega)|_{dB}$  in green, and  $|L(j\omega)|_{dB}$  in red—are shown on the loop shaping diagram in Fig.26. These graphs verify that  $|1/S(j\omega)|_{dB} \approx |L(j\omega)|_{dB}$  when  $\omega < 4$  rad/s and  $|T(j\omega)|_{dB} \approx |L(j\omega)|_{dB}$  when  $\omega > 20$  rad/s. The controller designer would like to make  $|L(j\omega)|_{dB}$  large (i.e., to decrease  $|S(j\omega)|$ ) in the low frequency range and at the same time make  $|L(j\omega)|_{dB}$  small (i.e., to decrease  $|T(j\omega)|$ ) in the high frequency range.

The high frequency portion ( $\omega > 6$  rad/s) of the  $|T(j\omega)|_{dB}$  graph was employed in Ex 13 and Ex 15 to respectively obtain the generalized stability margin function  $\mathcal{M}(\omega)$  and the gain/phase margins.

In the low frequency portion of the  $|L(j\omega)|_{dB}$  or  $|1/S(j\omega)|_{dB}$  graph, for instance, when  $\omega = 1$  rad/s, we have

$$|L(j1)|_{dB} = |1/S(j1)|_{dB} = 26 \text{ dB} \rightarrow |S(j1)| = 0.05$$

which means the tracking error of the reference input signal at the frequency  $\omega = 1$  rad/s will be only 5%. Similarly, when  $\omega = 0.1$  rad/s, we have

$$|L(j0.1)|_{dB} = |1/S(j0.1)|_{dB} = 46 \text{ dB} \rightarrow |S(j0.1)| = 0.005$$

which means the tracking error of the reference input signal at the frequency  $\omega = 0.1$  rad/s will be only 0.5%.

The loop shaping graphs on Figure 9.26 are obtained using the following MATLAB code:

```
% Fig9.26 CSD_LoopShaping_Ex9.26
num=5000; den=[1 55 250 0]; L=tf(num,den);
% Complementary function T
T = feedback(L,1);
% Sensitivity function S
S=1-T;
figure(34),
sigma(inv(S), 'b', T, 'g', L, 'r', {.1,100}),
grid on
```